

Research paper

Solid molecular dispersions of poorly water-soluble drugs in poly(2-hydroxyethyl methacrylate) hydrogels

Payam Zahedi, Ping I. Lee *

Department of Pharmaceutical Sciences, University of Toronto, Toronto, ON, Canada

Received 1 August 2006; accepted in revised form 30 October 2006

Available online 19 December 2006

Abstract

The applicability of cross-linked hydrogels in forming solid molecular dispersions to enhance the delivery of poorly soluble drugs has not been fully explored. The purpose of this study is to characterize physicochemical parameters affecting the formation of solid molecular dispersions of poorly water-soluble drugs in poly(2-hydroxyethyl methacrylate) (PHEMA) hydrogels and to investigate the effect of storage humidity levels on their physical stability. Samples were prepared by an equilibrium solvent loading process, using diclofenac sodium, piroxicam and naproxen as model drugs. These were characterized by X-ray diffraction (XRD), differential scanning calorimetry (DSC) and Fourier transform infrared spectroscopy (FTIR), as well as changes in the physical state during storage under different humidity conditions. The results show that a threshold drug loading level of about 30% exists in these solid molecular dispersions, above which amorphous to crystalline transition may occur. At any given drug loading, the onset of such change in physical state is accelerated at higher relative humidity levels during storage. The presence of hydrogen bonding between the polymer and the drug, as reflected in the observed FTIR band shifts, improves the compatibility between the drug and the polymer. This, together with a decreased mobility in the glassy polymer, helps to retard the crystallization event below the loading threshold. An increase in dissolution rate is also observed from the polymeric solid molecular dispersion as compared with that of the crystalline pure drug. These physicochemical results indicate that solid molecular dispersions based on PHEMA hydrogels can effectively enhance the dissolution and therefore should be potentially useful in improving the oral bioavailability of poorly water-soluble drugs.

© 2006 Elsevier B.V. All rights reserved.

Keywords: Solid dispersion; Poly(2-hydroxyethyl methacrylate); Hydrogel; Poorly water-soluble drug; Solubility enhancements; Physicochemical characterization; Storage stability; Effect of relative humidity; Dissolution

1. Introduction

One major challenge in the oral drug delivery area has been the low bioavailability of many compounds exhibiting poor solubility characteristics. With the advent of high throughput screening in drug discovery, the number of poorly water-soluble drug candidates has increased significantly [1]. As a result, the enhancement of bioavailability of these compounds has become one of the major challenges

in drug development. Among various methods employed to improve the rate of dissolution for poorly water-soluble drugs, the preparation of solid molecular dispersions (or solid solutions) in pharmaceutically acceptable water-soluble polymers such as polyvinylpyrrolidone (PVP) has been shown to be particularly effective in enhancing the rate of dissolution and the oral bioavailability. This is a result of the higher aqueous solubility of the amorphous drug in the solid molecular dispersion which generates a transiently supersaturated solution, thereby, enhancing the driving force for absorption [2–5].

Despite the fact that the utility of solid molecular dispersion has been known for many years, it has only been employed in a handful of commercial products [6]. Other than being limited by the complexity in the method of

* Corresponding author. Department of Pharmaceutical Sciences, Leslie Dan Faculty of Pharmacy, University of Toronto, 144 College Street, Toronto, ON, Canada M5S 3M2. Tel.: +1 416 946 0606; fax: +1 416 978 8511.

E-mail address: ping.lee@utoronto.ca (P.I. Lee).

preparation and manufacturing scale up (e.g., spray drying from organic solvents, hot melt extrusion, etc.) as well as the reproducibility of its physicochemical properties, the lack of a wider commercial application is mainly a result of long-term stability issues such as the appearance of crystalline drug and the resulting decrease in dissolution rate on aging of the amorphous solid molecular dispersion. To be able to take full advantage of this promising approach to improve bioavailability for poorly water-soluble drugs, it is necessary to establish a more in-depth understanding of physicochemical factors affecting, and criteria determining, the physical state and stability of such amorphous systems.

The mechanism of crystallization inhibition in solid molecular dispersions is not completely understood. Factors such as reduced molecular mobility in polymers with high glass transition temperatures (T_g), change in the interfacial energy and specific hydrogen-bonding interaction between the drug and polymer have been identified in the pharmaceutical literature as responsible for the inhibition of drug crystallization in amorphous drug-PVP solid solutions/dispersions [7–11]. However, the effect of humidity level on the stability of such systems has not been investigated to any great extent in terms of time-dependent changes in the state of the entrapped drug. Another inadequately understood aspect involves factors determining the maximum level of amorphous drug that can be safely incorporated into the polymer without risking crystallization during storage. A better understanding of such governing physicochemical factors therefore becomes essential in devising new strategies to enhance the long-term stability of such amorphous solid dispersion systems.

Despite the interest in using water-soluble polymers in forming solid molecular dispersions, the application of cross-linked glassy hydrogels to stabilize entrapped drug in an amorphous state for the purpose of enhancing the dissolution and bioavailability of poorly soluble drugs has not been fully explored. Such hydrogel systems will be the focus of the present study. Cross-linked glassy hydrogels, especially those based on polymers or copolymers of 2-hydroxyethyl methacrylate (HEMA), are generally inert and biocompatible with a history of clinical use in drug delivery systems and contact lenses [12–14]. The major advantage of using cross-linked hydrogels rather than water-soluble polymers to form solid molecular dispersions of poorly soluble drugs lies in its ease of manufacture and the substantial reduction of organic solvent emission associated with conventional spray drying of solid dispersions based on soluble polymers such as PVP. In addition, these cross-linked hydrogels are inert and insoluble, and therefore will not be absorbed in oral delivery applications. Previous studies on hydrogel controlled release systems by Lee [12,15] suggest that amorphous dissolved or dispersed drug can be readily formed in cross-linked hydrogels as a result of the unique equilibrium drug loading process, and a threshold loading concentration exists above which drug crystallization may occur in the

polymer. Throughout this manuscript, the term “amorphous dissolved” is intended to indicate amorphous drug that is dissolved in the polymer as opposed to being dispersed. In this study, we focus on the aspect of solubility and dissolution rate enhancement and examine in detail physicochemical parameters affecting the state of poorly water-soluble model drugs molecularly dispersed in PHEMA hydrogels. In particular, the effect of storage humidity condition on the stability of such solid molecular dispersions is also assessed.

2. Materials and methods

2.1. Materials

2-Hydroxyethyl methacrylate 98% (HEMA) and ethylene glycol dimethacrylate 98% (EGDMA), both obtained from Sigma–Aldrich Canada, were distilled under vacuum prior to use to remove the hydroquinone inhibitor. Methyl methacrylate 99% (MMA), from Fluka Germany, was purified to remove hydroquinone stabilizer by adsorption with aluminum oxide powder. Benzoyl peroxide, diclofenac sodium salt, naproxen, and piroxicam were purchased from Sigma–Aldrich Canada and used without further purification. All other chemicals were reagent grade obtained commercially and used as received.

2.2. Polymer synthesis

PHEMA sheets of various cross-linking agent concentrations (0.5, 0.66, 1, 3, 5, 10 mol%) and copolymers of HEMA with different MMA content (10, 20, 40, 50% v/v) at a fixed cross-linking agent concentration of 0.66 mol% were synthesized by free radical bulk polymerization using 0.1 mol% of benzoyl peroxide as the initiator and EGDMA as the cross-linking agent. Monomer mixtures were injected into a custom mold consisting of two glass plates lined with Mylar sheets (0.003 in.), separated by a silicon rubber spacer (0.06 in.) and held together with multiple binder clips. The polymerization was carried out at 80 °C for 3 h followed by 1 h at 100 °C to decompose any remaining initiator. After the completion of polymerization, the hydrogel sheets were extracted in a 50:50 water:methanol (v/v%) bath for 2 days to remove any unreacted extractables. After further equilibration in distilled water, circular disc samples were cut from the swollen hydrogel sheets followed by drying at 50 °C under vacuum over a 24 h period. The dried discs (average diameter of 0.31 in.) were stored in desiccators before use.

For the dissolution comparison study, PHEMA beads of 180–230 μm size range were synthesized by suspension polymerization of HEMA monomer with 0.66 mol% of EGDMA as the cross-linking agent and 0.1% mol/mol of benzoyl peroxide as the initiator according to previously reported procedures [12]. Afterwards, the PHEMA beads were extracted in a Soxhlet with methanol for 2 days, dried

at 50 °C under vacuum for 24 h, before being fractionated and stored in desiccators until use.

2.3. Polymer swelling characterization

Equilibrium swelling properties of hydrogel discs were determined gravimetrically at 25 °C. The swelling ratio q was calculated by:

$$q = \frac{W_s}{W_d} \quad (1)$$

where W_s represents the swollen weight of the sample and W_d is the dry weight of the sample before swelling. The equilibrium water (or solvent) content (EWC), which represents the solvent weight percentage within the swollen polymer [13], was calculated from:

$$\text{EWC}(\%) = 100 \times \left(\frac{W_s - W_d}{W_s} \right) \quad (2)$$

2.4. Model drug selection

The model drugs used in preparing the solid molecular dispersions for this study were diclofenac sodium salt (DSS), naproxen (NAP) a weak acid, and piroxicam (PIR) a weak base, all of which are non-steroidal anti-inflammatory drugs (NSAIDs) [16]. NSAIDs act as non-selective inhibitors of the enzyme cyclooxygenases, required for the production of prostaglandins, which are involved in the inflammation process [17]. They generally have very low aqueous solubility but are more soluble in organic solvents

[18–20]. The physical and chemical properties of these three model drugs are summarized in Table 1. Most of the data reported here were generated with the model drug DSS. Additional results using NAP and PIR as model drugs were also obtained to illustrate certain general trends.

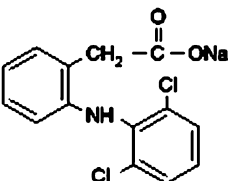
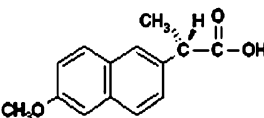
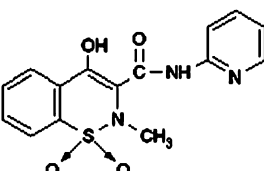
2.5. Preparation of solid molecular dispersions

The following solvents were used for loading drugs into the polymer matrix: 90:10 ethanol:water (v/v%) for DSS; 100% ethanol for NAP; and 100% acetone for PIR. The polymer discs were equilibrated in loading solutions with a range of different drug concentrations. After removal from the loading solution the drug loaded polymer discs were blotted with filter paper to remove any excess liquid on the sample surface before being dried at 50 °C under vacuum for 24 h. The drug loading levels in the resulting dried samples were determined gravimetrically and the samples were stored in desiccators before analysis.

2.6. Aqueous drug solubility

Each drug was recrystallized to remove any potential amorphous regions developed during any prior processing and size reduction. The recrystallization was carried out in water for DSS, methanol for NAP and acetone for PIR. Solubility of each drug was measured in both distilled water (pH 5.1) and phosphate buffer (pH 7.2). An excess amount of recrystallized drug was allowed to equilibrate in the aqueous medium for 2 days. Drug concentration in the supernatant was analyzed on a Carry 50 UV–vis

Table 1
Physical and chemical properties of three model drugs

Structure	MW (g/ml)	pK _a	UV _{max} (nm)	Solubility	Ref.
 <p>Diclofenac sodium</p>	318.13	4	276 (water)	<ul style="list-style-type: none"> • Water (pH 5.2) >9 mg/ml • Methanol >24 mg/ml • Acetone 6 mg/ml • Phosphate buffer (pH 7.2) 6 mg/ml 	[18]
 <p>Naproxen</p>	230.26	4.2	271 (methanol)	<ul style="list-style-type: none"> • 25 parts ethanol (96%) • 20 parts methanol • 15 parts chloroform • 40 parts ether • Practically insoluble in water 	[19]
 <p>Piroxicam</p>	331.35	6.3	355 (acetone)	<ul style="list-style-type: none"> • Not soluble in water • Sparingly soluble in toluene • Only slightly more soluble in methanol, ethanol and isopropanol 	[20]

spectrophotometer (Varian, Ontario, Canada) at 276 nm for DSS, 271 nm for NAP, and 355 nm for PIR.

2.7. Dissolution testing

Dissolution comparison of the pure crystalline drug with drug-PHEMA solid molecular dispersion was conducted using the USP II paddle method. The average particle size of each drug was measured on a Motic BA400 optical microscope (Motic Instruments, Vancouver, Canada) using an image analysis software (Motic Image Plus 2.0). This was done to get a comparison between the size of the PHEMA beads and each drug. The average particle size was determined to be 7.3 μm for DSS, 7.4 μm for NAP and 4.5 μm for PIR.

Dissolution testing was performed on an ERWEKA USP DT600 dissolution apparatus (ERWEKA, Ontario, Canada) using 500 ml of 0.1 M phosphate buffer (pH 7.2) at $37 \pm 0.5^\circ\text{C}$ as the dissolution medium and a paddle speed of 100 rpm. At each predetermined time interval, 2 ml aliquot was removed and replaced with 2 ml fresh dissolution medium. Drug concentration in the aliquot was determined spectrophotometrically as described in the previous section. At least three measurements were run and averaged for each sample.

2.8. Stability studies

Stability testing on solid molecular dispersions was conducted by storing samples in sealed glass jars containing saturated salt solutions at 25°C . Five saturated salt solutions at various constant relative humidity (RH) levels were utilized: potassium acetate (22% RH), potassium carbonate (43% RH), sodium nitrite (64% RH), sodium chloride (75% RH) and potassium nitrate (92% RH). Changes in physical state of the samples after storage were followed visually over time and confirmed by DSC measurements.

2.9. X-ray diffractometry

A Philips X-ray diffraction (XRD) system (Phillips, Ontario, Canada) with basic components of PW 1830 HT generator, PW 1050 goniometer, PW3710 control electronics, and X-Pert system software was used to analyze the physical state of various samples. Each sample was mounted on a side-open sample holder. A scan rate of $1.2^\circ \text{min}^{-1}$ over a 2θ range of $5\text{--}35^\circ$ was used.

2.10. Thermal analysis

A TA Instruments Q100 differential scanning calorimetry (DSC) (TA Instruments, Delaware, USA) was used for sample thermal analysis. Samples (5–10 mg) were weighed into aluminum pans and cold-sealed. These samples were heated or cooled at a rate of $5^\circ\text{C}/\text{min}$ under nitrogen purge.

2.11. Fourier transform infrared spectroscopy

Fourier transform infrared (FTIR) spectra were obtained on a universal Attenuated Total Reflectance (ATR) Spectrum-one Perkin-Elmer spectrophotometer (Perkin-Elmer, Connecticut, USA). The spectra were recorded from 4000 to 650 cm^{-1} . All spectra were collected as an average of 20 scans at a resolution of 2 cm^{-1} .

3. Results and discussion

3.1. Polymer swelling characteristics

The degree of equilibrium swelling of a hydrogel is one of its most important properties because it determines the rates of water sorption and drug release, mechanical strength, and biocompatibility [13]. Factors such as the hydrophilicity of polymer, degree of cross-linking and concentration of ionizable functional groups in the network (if any) determine the level of swelling. For example, it is well known that the average molecular weight between cross-links and the resulting equilibrium solvent swelling in PHEMA hydrogels will decrease with increasing cross-linking ratio [21].

To correlate with the observed trend in drug loading capability, a comparison of the swelling behavior of PHEMA in the present loading solvent with that in water is necessary. Fig. 1 illustrates the equilibrium swelling of PHEMA in the loading solvent (90:10 ethanol:water) and in water as a function of the polymer cross-linking ratio. A general decrease in the equilibrium swelling is seen with increasing cross-linking ratios (from 0.005 to 0.1) with a bigger reduction in the loading solvent swelling (from 57.0% to 23.6%) than the water swelling (from 36.5% to 21.7%). On the other hand, increasing the amount of hydrophobic MMA in the copolymer from 0% to 50% v/v leads to only minute changes in equilibrium swelling in the loading solvent (from 56.5% to 53.5%) as compared

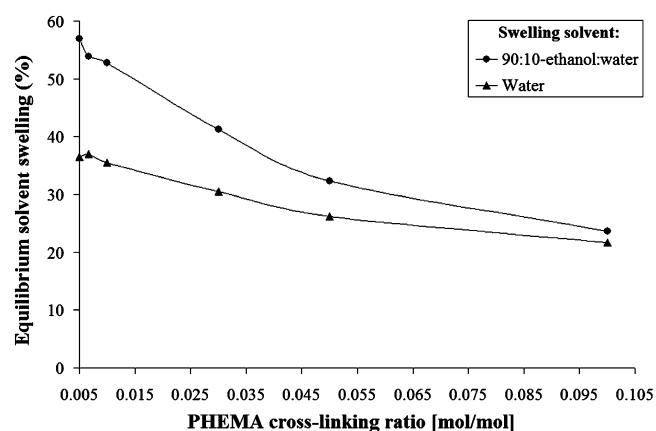


Fig. 1. Equilibrium swelling of PHEMA hydrogel discs at 25°C as a function of cross-linking ratio and solvent type.

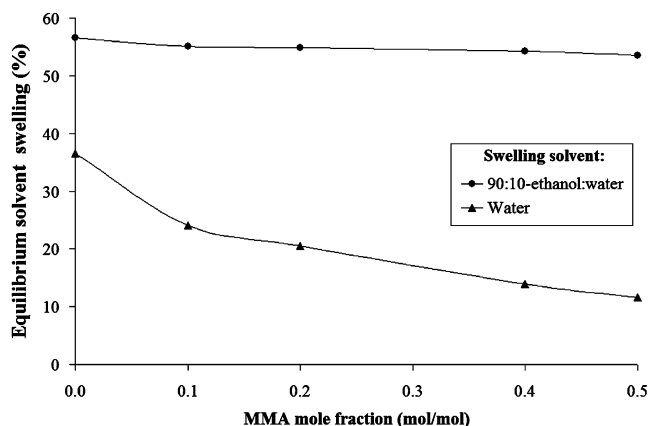


Fig. 2. Equilibrium swelling of P(HEMA-co-MMA) hydrogel discs at 25 °C as a function of MMA content and solvent type.

to that in water swelling (from 36.5% to 11.6%) as shown in Fig. 2.

3.2. Drug loading and physical state of drug

Fig. 3a illustrates the effect of increasing cross-linking density on final DSS drug loading in the PHEMA based solid molecular dispersions. Drug loading levels ranging

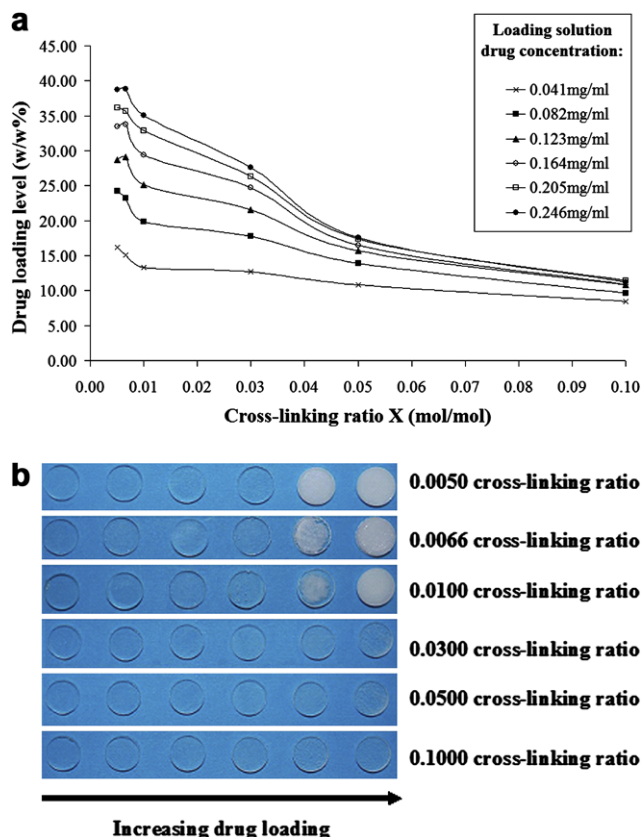


Fig. 3. Characteristics of DSS loaded PHEMA discs. (a) DSS drug loading level in PHEMA as a function of cross-linking ratio and loading solution concentration. (b) Photographs of corresponding DSS-PHEMA samples with evidence of threshold drug loading levels.

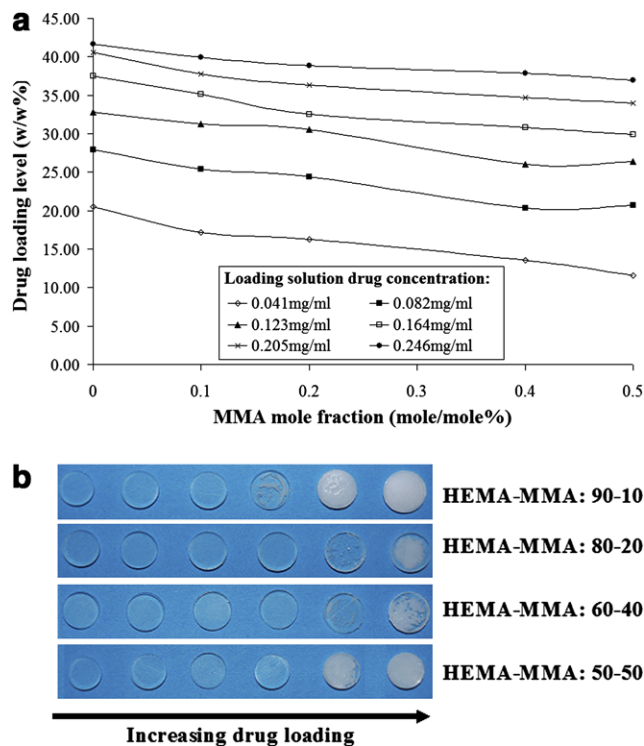


Fig. 4. Characteristics of DSS loaded P(HEMA-co-MMA). (a) DSS drug loading level in P(HEMA-co-MMA) as a function of MMA content and loading solution concentration. (b) Photographs of corresponding DSS-P(HEMA-co-MMA) samples with evidence of threshold drug loading levels.

from about 8% to 40% w/w are attained. In general, for any given loading solution concentration, the corresponding DSS drug loading level decreases with increasing cross-linking density as a result of decreasing number average molecular weight between cross-links and a reduction in equilibrium swelling in the loading solvent (see Fig. 1). Similarly, Fig. 4a shows the DSS drug loading levels (ranging from 11% to 41% w/w) as a function of the MMA content in the P(HEMA-co-MMA) discs at a fixed cross-linking agent concentration of 0.66 mol%. An increase in MMA content leads to only slight decrease in drug loading levels due to the relatively small change in polymer swelling in the loading solvent (see Fig. 2). Furthermore, a transition from optically clear discs to opaque discs above a certain threshold drug loading is observed in PHEMA with low cross-linking ratios ($0.01 \leq$) and in P(HEMA-co-MMA) with MMA content up to 50% as illustrated in photographs of Figs. 3b and 4b. It can be seen that the threshold level occurs at about 30–33% drug loading and it appears to be only slightly decreased with increasing polymer cross-linking ratio or the MMA content. A more precise determination of this threshold level and its trend is not feasible from the present data because of the discrete drug loading levels studied. This change in sample appearance is a result of the loaded drug converting from an amorphous dissolved state to a crystalline dispersion above a certain threshold loading

level. Such transition is less desirable for enhancing the solubility of poorly water-soluble drugs because the crystalline state has a slower rate of dissolution [11] and lower solubility than the amorphous form [22]. On the other hand, no such clear to opaque transition is observed in PHEMA samples with cross-linking ratios larger than 0.01 because the maximum achievable loading levels in these samples are all below the observed threshold (see Figs. 3a and b). Similarly, the achievable drug loading levels for NAP in PHEMA range from 11% to 17% w/w and for PIR in PHEMA from 5% to 10% w/w. These NAP-PHEMA and PIR-PHEMA solid molecular dispersion samples remain optically clear without any detectable transition in the drug loading range studied (photographs not shown). The optical clarity of the hydrogel samples provides a direct indication of a potential transition between the amorphous dissolved and crystalline precipitated states, which cannot be observed easily in the conventional spray-dried solid molecular dispersions based on soluble polymers such as PVP.

XRD and DSC provide a systematic way to verify the final state of the overall solid molecular dispersion. The

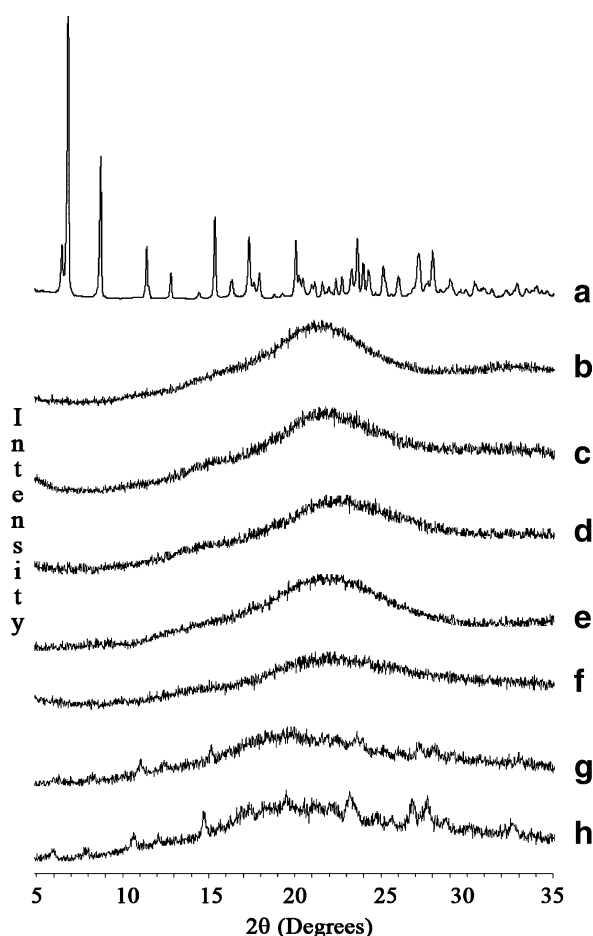


Fig. 5. XRD patterns of DSS loaded PHEMA. (a) DSS; (b) PHEMA; (c) DSS-PHEMA: 15.1%; (d) DSS-PHEMA: 23.3%; (e) DSS-PHEMA: 29.1%; (f) DSS-PHEMA: 33.8%; (g) DSS-PHEMA: 35.7%; (h) DSS-PHEMA: 38.8%.

XRD patterns for DSS-PHEMA solid molecular dispersions are shown in Fig. 5. The sharp peaks associated with pure DSS (Fig. 5a) are characteristic of its crystalline form. On the other hand, the pure PHEMA polymer exhibits a typical broad amorphous band (Fig. 5b). As the drug loading level increases some of the characteristic peaks of crystalline DSS gradually emerge, especially above 30% drug loading, suggesting an increase in crystallinity in these solid molecular dispersions. The absence of diffraction peaks below this drug loading level confirms that the DSS is present in an amorphous form within the already amorphous PHEMA matrix. Therefore, the glassy PHEMA matrix inhibits the in situ recrystallization of DSS. On the other hand, the XRD patterns for NAP-PHEMA and PIR-PHEMA do not show any characteristic diffraction peaks in the loading range studied (below 10% and 20%, respectively) suggesting the presence of amorphous solid molecular dispersions (data not shown) below the threshold drug loading level.

Typical DSC thermograms of DSS-PHEMA solid molecular dispersions are displayed in Fig. 6 where DSS shows a melting endotherm at 291 °C, whereas no melting peaks exist for pure PHEMA or at low loading levels of DSS. As the loading level of DSS in PHEMA exceeds about 30%, broadened melting peaks appear. However, these peaks occur at a lower temperature compared to the pure DSS melting peak. This may be due to a low melting polymorph of the drug being formed in the polymer. Although both the sample scan rate and the environmental atmospheric condition can drastically affect the DSC thermogram of DSS [23], an effort was made to maintain these parameters constant in this study. It is worth noting that no such visible DSC melting peaks were seen in the

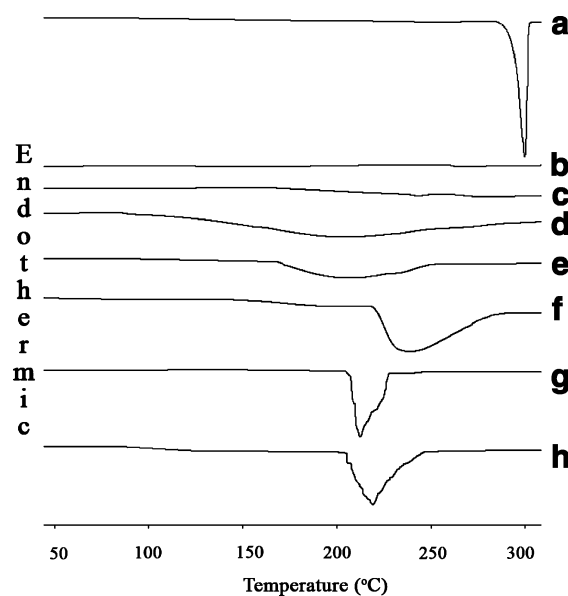


Fig. 6. DSC thermograms of DSS loaded PHEMA. (a) DSS; (b) PHEMA; (c) DSS-PHEMA: 15.1%; (d) DSS-PHEMA: 23.3%; (e) DSS-PHEMA: 29.1%; (f) DSS-PHEMA: 33.8%; (g) DSS-PHEMA: 35.7%; (h) DSS-PHEMA: 38.8%.

NAP-PHEMA and PIR-PHEMA solid molecular dispersions (data not shown) where the drug loading levels (less than 10% and 20%, respectively) are well below the threshold loading level of approximately 30% seen with DSS-PHEMA. This lack of a melting endotherm is due to the drug being present in an amorphous dissolved phase in the polymer matrix.

3.3. Polymer–drug interactions

FTIR was employed to study the physiochemical interactions between the drug and polymer in drug-loaded PHEMA hydrogels. In all three drug–polymer combinations studied, there is a clear evidence of the presence of hydrogen bonding between the drug and polymer. This intermolecular interaction improves the compatibility between the drug and the polymer. Together with the decreased mobility in a glassy polymer, they help to retard the nucleation and crystallization event. The crystallization of drug from supersaturated solution consists of two processes: appearance of crystal nucleus and growth of the crystal [24]. Hence, the presence of the glassy PHEMA matrix inhibits the crystallization of dissolved drug in the solid molecular dispersion, where the drug is present in an amorphous dissolved state. However, it must be noted that the drug loading level can influence the extent of such inhibitory effect in the polymer since an increase in drug loading effectively also reduces the polymer concentration. In fact above a threshold loading level (or below a threshold polymer concentration), the drug precipitates out in fine crystalline form. In the case of DSS, this transition drug loading level appears to be around 30% as discussed above.

Fig. 7 shows the FTIR spectra for DSS-PHEMA, NAP-PHEMA and PIR-PHEMA solid molecular dispersions as a function of drug loading level. The existence of hydrogen bonding is reflected by band shifts seen in the spectra associated with key functional groups of the drugs which interact with the hydroxyl groups of PHEMA (3345 cm^{-1}). The aforementioned functional groups are: —NH (3380 and 1499 cm^{-1}) in DSS, —COO (3180 and 1726 cm^{-1}) in NAP and —NH in PIR (3385 and 1435 cm^{-1}). Examples of the observed band shifts include $1499\text{--}1501\text{ cm}^{-1}$ for DSS-PHEMA samples and $1726\text{--}1723\text{ cm}^{-1}$ for NAP-PHEMA samples.

3.4. Dissolution comparison

The aqueous solubilities at $25\text{ }^{\circ}\text{C}$ for DSS, NAP and PIR are: 15.8 , 0.07 and 0.12 mg/ml , respectively, in distilled water (pH 5.1) and 5.6 , 1.8 and 0.54 mg/ml , respectively, in phosphate buffer (pH 7.2). The prospect of enhancing the dissolution is best illustrated with solid molecular dispersions of the two least soluble model drugs, NAP and PIR. Figs. 8a and b compare the dissolution profiles of NAP-PHEMA and PIR-PHEMA solid molecular dispersions with that of the crystalline pure drug. It is apparent

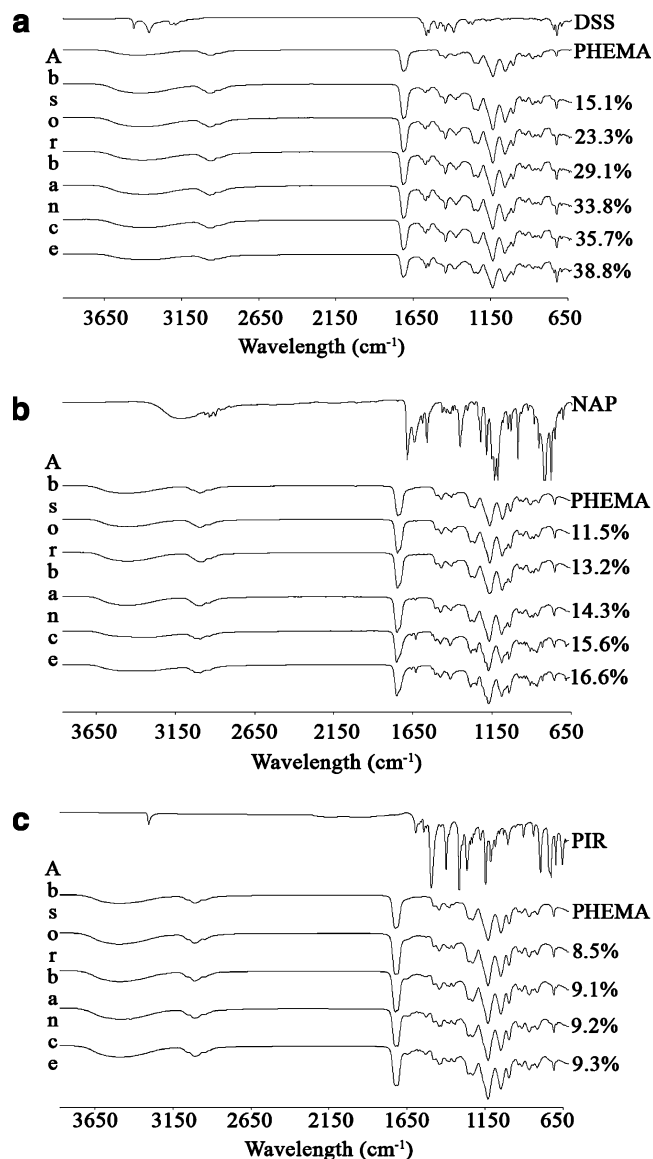


Fig. 7. FTIR spectra of drug loaded PHEMA. (a) DSS system. (b) NAP system. (c) PIR system.

that the rate of dissolution is faster from the solid molecular dispersion compared to that of the crystalline pure drug despite the fact that both crystalline pure drugs have much smaller average particle sizes than their corresponding solid molecular dispersions based on PHEMA beads ($7.4\text{ }\mu\text{m}$ or $4.5\text{ }\mu\text{m}$ versus $180\text{--}230\text{ }\mu\text{m}$). In other words, although faster drug dissolution is normally expected from smaller particles, the dissolution rate of a solid molecular dispersion of PIR from PHEMA beads has been enhanced to the point that it surpasses the dissolution of crystalline PIR, resulting in an overall faster dissolution (Fig. 8b). Again, this is primarily because the drug is present in an amorphous dissolved form in the solid molecular dispersion having a higher transient aqueous solubility than its crystalline pure form. On the other hand, the closeness of the observed dissolution profiles for NAP solid molecular dispersion versus that of the crystalline pure drug (Fig. 8a) is a direct

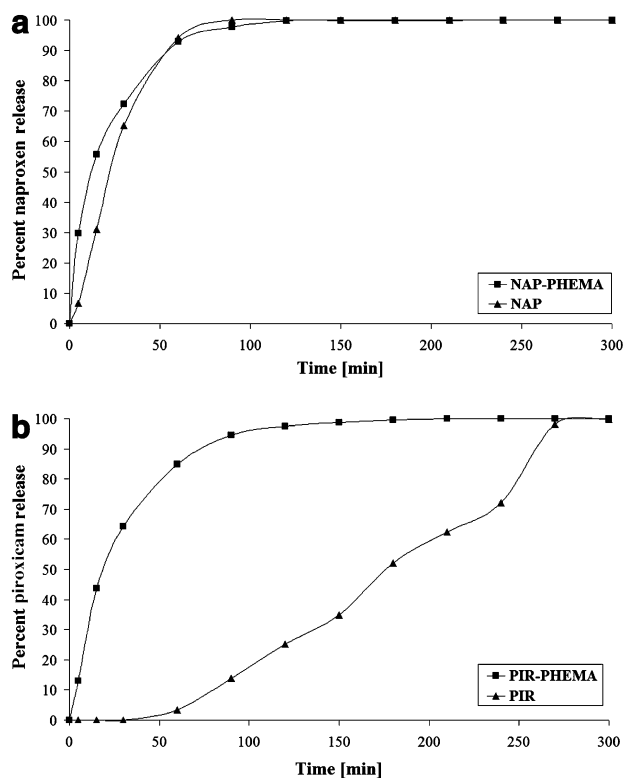


Fig. 8. Dissolution profiles comparing pure crystalline drug to drug-PHEMA solid molecular dispersions. (a) NAP versus NAP-PHEMA (13% w/w loading level). (b) PIR versus PIR-PHEMA (9% w/w loading level).

result of increased solubility and rate of dissolution of NAP in the dissolution medium. In this case, the enhanced dissolution from solid molecular dispersion of NAP in PHEMA beads appears to be only slightly better than that from the smaller crystalline pure drug particles. For the most soluble model drug, DSS, there is still an enhancement of dissolution from its solid molecular dispersion, however the larger PHEMA particle size makes such advantage in dissolution rate less obvious when compared with the dissolution from crystalline pure drug of much smaller particle sizes (results not shown).

3.5. Storage stability outcome

Fig. 9 illustrates the changes seen in DSS-PHEMA solid molecular dispersions stored at various humidity levels. The drug loading levels of the DSS-PHEMA samples were all at 26% w/w. As the relative humidity of the storage

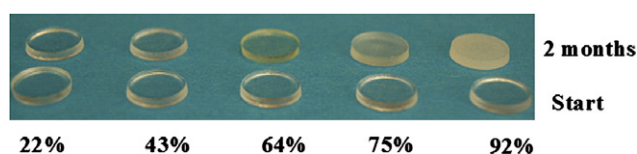


Fig. 9. Changes observed in DSS-PHEMA discs during storage stability at 25 °C and various humidity levels over a 2 months period. All samples had a drug loading level of 26% w/w.

Table 2

Summary of stability testing under various humidity levels at 25 °C over 2 months

RH (%)	DSS-PHEMA	NAP-PHEMA
22	No change	No change
43	No change	No change
64	34 days	No change
75	12 days	18 days
92	3 days	3 days

Time of change represents the onset of transformation from a clear to an opaque sample. Drug loading: 26% in DSS-PHEMA; 13% in NAP-PHEMA.

environment increases, the onset of transition from a clear sample to an opaque one is accelerated. This is manifested by phase separation in the presence of moisture. At lower humidity levels, the plasticizing effect and the phase separation tendency in the solid molecular dispersion will decrease due to reduced mobility in the glassy PHEMA matrix. Thus, the solid molecular dispersion remains in the amorphous form longer. Table 2 summarizes the observed onset time of physical changes in the DSS-PHEMA and NAP-PHEMA solid molecular dispersions (with loading levels of 26% w/w and 13% w/w, respectively). The onset of physical changes at different humidity levels appears to be faster for DSS-PHEMA solid molecular dispersions than for NAP-PHEMA solid molecular dispersions primarily due to the higher DSS drug loading levels.

Fig. 10 illustrates the DSC thermograms for DSS-PHEMA sample discs stored at 92% relative humidity. Prior to exposure to the high humidity level, no melting endotherm is seen in the DSS-PHEMA sample indicating the presence of an amorphous solid molecular dispersion (Fig. 10c). However after storage at 92% relative humidity for 3 days, the sample exhibits a distinctive melting peak associated with the crystalline drug. At a lower relative humidity such

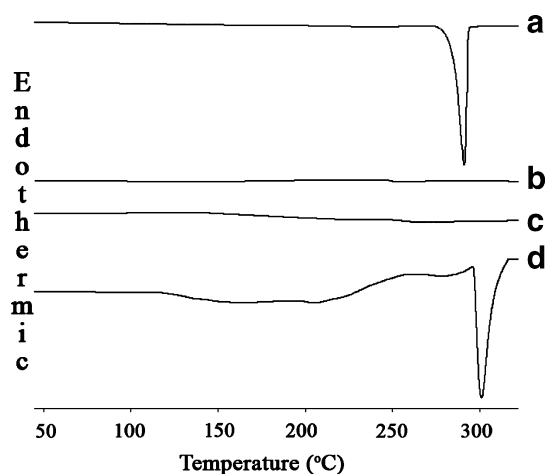


Fig. 10. DSC thermograms of DSS-PHEMA stability samples. (a) DSS reference; (b) PHEMA reference; (c) DSS-PHEMA before stability testing; (d) DSS-PHEMA after 3 days at 92% RH.

as 22%, no visible change was seen over a 2 months period as confirmed by DSC measurements (data not shown).

4. Conclusion

Based on the physicochemical results obtained here, PHEMA based hydrogels can serve as effective carriers for solid molecular dispersions of poorly water-soluble drugs. The glassy hydrogel matrix hinders the crystallization of poorly water-soluble drugs dissolved in the polymer matrix. A threshold drug loading level exists, above which amorphous to crystalline transition tends to occur. This transition is accelerated at higher humidity levels. Several factors are found to influence the final state of the drug within the polymer. These are the extent of polymer cross-linking and hydrophobic co-monomer content which affect the achievable drug loading levels, and the storage humidity condition which affects the hydration and phase separation within the hydrogel network. An enhancement in drug dissolution rate has been observed from the solid molecular dispersions as compared to the crystalline pure drug. With demonstrated improvements in drug solubility and dissolution rate as reported in this study, solid molecular dispersions based on cross-linked glassy hydrogels should be potentially useful in improving the oral bioavailability of poorly water-soluble drugs.

Acknowledgments

This work was supported in part by the Leslie Dan Faculty of Pharmacy, University of Toronto and the Canadian Institute of Health Research (DRC-68179). Special thanks are due to Dr. C. Allen for allowing access to her DSC and FTIR equipment and to Mr. Yin Ma for providing suspension polymerized PHEMA beads.

References

- [1] C.A. Lipinski, F. Lombardo, B.W. Dominy, P.J. Feeney, Experimental and computational approaches to estimate solubility and permeability in drug discovery and development settings, *Adv. Drug Deliv. Rev.* 23 (1997) 3–25.
- [2] O.I. Corrigan, R.F. Timoney, M.J. Whelan, The influence of polyvinylpyrrolidone on the dissolution and bioavailability of hydrochlorothiazide, *J. Pharm. Pharmacol.* 28 (1976) 703–706.
- [3] C. Leuner, J. Dressman, Improving drug solubility for oral delivery using solid dispersions, *Eur. J. Pharm. Biopharm.* 50 (2000) 47–60.
- [4] S.A. Sangekar, P.I. Lee, W.A. Vadino, Solid solution of an antifungal agent with enhanced bioavailability, U.S. Patent 5,972,381, 1999.
- [5] S.A. Sangekar, P.I. Lee, A.A. Nomeir, Molecular dispersion composition with enhanced bioavailability, U.S. Patent 6,632,455, 2003.
- [6] A.T.M. Serajuddin, Solid dispersion of poorly water-soluble drugs: early promises, subsequent problems, and recent breakthroughs, *J. Pharm. Sci.* 88 (1999) 1058–1066.
- [7] L.S. Taylor, G. Zografi, Spectroscopic characterization of interactions between PVP and indomethacin in amorphous molecular dispersions, *Pharm. Res.* 14 (1997) 1691–1698.
- [8] T. Matsumoto, G. Zografi, Physical properties of solid molecular dispersions of indomethacin with poly(vinylpyrrolidone) and poly(vinylpyrrolidone-co-vinylacetate) in relation to indomethacin crystallization, *Pharm. Res.* 16 (1999) 1722–1728.
- [9] K.J. Crowley, G. Zografi, The effect of low concentrations of molecularly dispersed poly(vinylpyrrolidone) on indomethacin crystallization from the amorphous state, *Pharm. Res.* 20 (2003) 1417–1422.
- [10] K. Khougaz, S.D. Clas, Crystallization inhibition of solid dispersions of MK-0591 and poly(vinylpyrrolidone) polymers, *J. Pharm. Sci.* 89 (2000) 1325–1334.
- [11] R. Nair, S. Gonen, S.W. Hoag, Influence of polyethylene glycol and povidone on the polymorphic transition and solubility of carbamazepine, *Int. J. Pharm.* 240 (2002) 11–22.
- [12] P.I. Lee, Kinetics of drug release from hydrogel matrices, *J. Control. Release* 2 (1985) 277–288.
- [13] S.H. Gehrke, Synthesis and properties of hydrogels used for drug delivery, in: G.L. Amidon, P.I. Lee, E.M. Topp (Eds.), *Transport Processes in Pharmaceutical Systems*, Marcel Dekker, New York, 2000, pp. 473–546.
- [14] A.S. Hoffman, Hydrogels for biomedical applications, *Adv. Drug. Deliv. Rev.* 43 (2002) 3–12.
- [15] P.I. Lee, C.J. Kim, Probing the mechanisms of drug release from hydrogels, *J. Control. Release* 16 (1991) 229–236.
- [16] M.D. Murray, D.C. Brater, Nonsteroidal anti-inflammatory drugs, *Clin. Geriatr. Med.* 6 (1990) 365–397.
- [17] J.R. Vane, R.M. Botting, New insights into the mode of action of anti-inflammatory drugs, *Inflamm. Res.* 44 (1995) 1–10.
- [18] C.M. Adeyeye, P.K. Li, Diclofenac sodium, in: K. Florey (Ed.), *Analytical Profiles of Drug Substances*, vol. 19, Academic Press, New York, 1990, pp. 123–144.
- [19] F.J. Al-Shammary, N.A.A. Mian, M.S. Mian, Naproxen, in: K. Florey (Ed.), *Analytical Profiles of Drug Substances*, vol. 21, Academic Press, New York, 1992, pp. 345–374.
- [20] M. Mihalic, H. Hofman, J. Kuftinec, B. Krile, V. Caplar, F. Kajfez, N. Blazevic, Piroxicam, in: K. Florey (Ed.), *Analytical Profiles of Drug Substances*, vol. 15, Academic Press, New York, 1986, pp. 509–532.
- [21] N.A. Peppas, H.J. Moynihan, L.M. Lucht, The structure of highly crosslinked poly(2-hydroxyethyl methacrylate) hydrogels, *J. Biomed. Mater. Res.* 19 (1985) 397–411.
- [22] B.C. Hancock, M. Parks, What is the true solubility advantage for amorphous pharmaceuticals? *Pharm. Res.* 17 (2000) 397–404.
- [23] P. Tudja, M.Z.I. Khan, E. Meštrović, M. Horvat, P. Golja, Thermal behaviour of diclofenac sodium: decomposition and melting characteristics, *Chem. Pharm. Bull.* 49 (2001) 1245–1250.
- [24] V. Tantishaiyakul, N. Kaewnopparat, S. Ingkatawornwong, Properties of solid dispersions of piroxicam in polyvinylpyrrolidone, *Int. J. Pharm.* 181 (1999) 143–151.